subjected to boundary conditions:

$$R = R_w, \quad I = I_w \quad \text{on} \quad \Gamma_1 \tag{8}$$

and

$$\left.\begin{aligned} k_x \frac{\partial R}{\partial x} l_x + k_y \frac{\partial R}{\partial y} l_y &= q_R, \\ k_x \frac{\partial I}{\partial x} l_x + k_y \frac{\partial I}{\partial y} l_y &= q_I \end{aligned}\right\} \text{on} \quad \Gamma_2. \tag{9}$$

Therefore, problem (6), (2'), (3') is a special case of problem (7)–(9). Consequently the computer code described in [1] can be used, without modifications, for the analysis of combined free and forced convection in a fully developed laminar steady flow.

After the values of R and I are obtained, dimensionless temperature and velocity distributions can be computed from the formulae:

$$w = \frac{R+I}{2} L, \quad t = \left[\frac{I-R}{2(Ra)^{1/2}} - \frac{1}{Ra}\right] L \tag{10}$$

where [3–5]:

$$L = \iint \mathrm{d}A / \iint (w/L)\,\mathrm{d}A. \tag{11}$$

EXAMPLES OF APPLICATION

To assess the accuracy of the finite element code used, computations were carried out for a square duct. The geometry considered and the finite element mesh utilized are shown in Fig. 1. Because of the existing symmetry, the analysis is limited to a right-angled isosceles sector and natural (i.e. zero flux) boundary conditions are assumed on the internal sides.

In Table 1 numerical results for the Nusselt number Nu and the pressure gradient parameter L are compared with analytical solution [3]. As it can be seen, isoparametric elements yield a good agreement even if a relatively coarse mesh is used.

Temperature and velocity distribution over the square centerline are shown in Fig. 2. The results compare favourably with the most accurate calculations in [2], where a much larger number of nodal points was used.

To demonstrate the capabilities of the program in dealing with complex realistic problems, velocity and temperature distributions were computed for the geometries shown in Fig. 3. The resulting values of the Nusselt number Nu and of the pressure gradient parameter L for the two geometrical situations are reported in Table 2 as a function of the Rayleigh number.

REFERENCES

1. M. D. Mikhailov, G. Comini, S. Del Giudice and G. P. Runchi, Determination of thermal wave distributions by the finite element method, *Int. J. Heat Mass Transfer* **20**, 195–200 (1977).
2. A. L. Nayak and P. Cheng, Finite element analysis of laminar convective heat transfer in vertical ducts with arbitrary cross-sections, *Int. J. Heat Mass Transfer* **18**, 227–236 (1975).
3. M. Iqbal, S. A. Ansari and B. D. Aggarwala, Effect of buoyancy on forced convection in vertical regular polygonal ducts, *J. Heat Transfer* **92**, 237–244 (1970).
4. L. S. Han, Laminar heat transfer in rectangular channels, *J. Heat Transfer* **81**, 121–128 (1959).
5. M. Iqbal, B. D. Aggarwala and A. G. Fowler, Laminar combined free and forced convection in vertical non-circular ducts under uniform heat flux, *Int. J. Heat Mass Transfer* **12**, 1123–1139 (1969).

Int J. Heat Mass Transfer Vol. 21, pp. 1621–1624

0017-9310/78/1201-1621 $02.00/0

MEASUREMENT OF TRANSITION BOILING BOUNDARIES IN FORCED CONVECTIVE FLOW

H. S. RAGHEB and S. C. CHENG
Department of Mechanical Engineering, University of Ottawa, Ottawa, Ontario, Canada

and

D. C. GROENEVELD
Chalk River Nuclear Laboratories, Atomic Energy of Canada Limited, Chalk River, Canada

(*Received* 26 *January* 1978 *and in revised form* 8 *May* 1978)

INTRODUCTION

THE TRANSITION boiling heat-transfer mode may be viewed as a combination of unstable (vapor) film boiling and unstable nucleate boiling alternatively existing at any given location on a heated surface. The variation of heat-transfer rate with temperature is primarily a result of the change in the fraction of time that each boiling mode exists at a given location.

The transition boiling mode is most efficient at the boiling crisis point which represents its lower temperature boundary. Conditions here may be predicted by a variety of correlations. The higher temperature boundary of the transition boiling mode takes place at or near the minimum heat flux point where a change from transition boiling to pure film boiling takes place. Little is known about the boundary between transition boiling and film boiling except that it is influenced by flow conditions, fluid properties and surface properties [1, 2].

Knowledge of the temperature boundaries of the transition boiling mode is important in the prediction of the temperature–time history of a hot surface during quenching (e.g. during emergency core cooling of a nuclear reactor). The purpose of this investigation was to determine whether during the quenching process (1) the minimum heat flux corresponds to the initiation of liquid contact on a surface, and (2) whether the critical heat flux corresponds to the initiation of continuous liquid contact [3].

This study is believed to be novel in two ways (a) to the authors' knowledge, no other investigator has ever measured the boundary between film boiling and transition boiling under forced convective conditions, and (b) the probe design is uniquely suited to high temperature operation. Few relevant studies have been reported in the literature. Iida and Kobayasi [4] measured the variation of

near wall void in pool boiling with an electrical probe protruding in the coolant. Their study covered the complete boiling régime. Other investigators [5, 6] have measured transition boiling temperature oscillations with thermocouples mounted on the outer tube surface or embedded in the tube wall.

EXPERIMENTAL APPARATUS

Figure 1 shows schematically the construction and installation details of the probe. The probe is made of a 1 mm zirconium wire insulated electrically from the test section by a zirconium oxide layer formed by autoclaving. To avoid corrosion of the probe tip during the high temperature operation in a steam atmosphere, a platinum coating was applied to the tip by a sputtering process under vacuum conditions.

Figure 2 shows a schematic diagram of the probe circuit. The probe can detect the presence of a slightly conducting liquid on the heated surface by using the platinum probe tip and the heating surface as the two electrodes. If the wall is dry, the resistance across AB is very large; therefore, a small voltage drop will be registered across CD. However, if the wall is wet, the resistance across AB is much smaller and a larger voltage drop across CD is noticed.

The test section with the probe and adjacent thermocouple installed is shown in Fig. 3. It consists of a 10.16 cm OD, 10.48 cm long, insulated copper cylinder having a central flow channel of 1.27 cm dia. Two 300 W, 0.635 cm diameter cartridge heaters are installed in the copper cylinder along with the probe and a thermocouple as shown in Fig. 3.

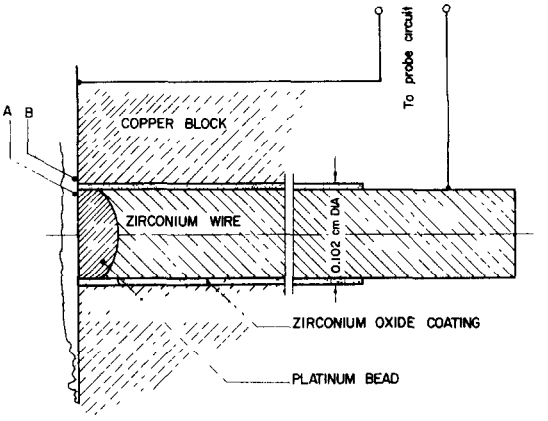

FIG. 1. Probe configuration.

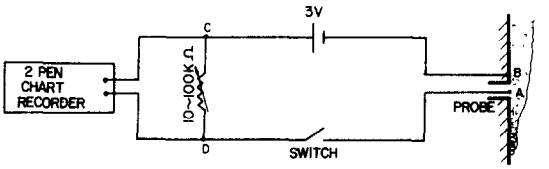

FIG. 2. Probe circuit.

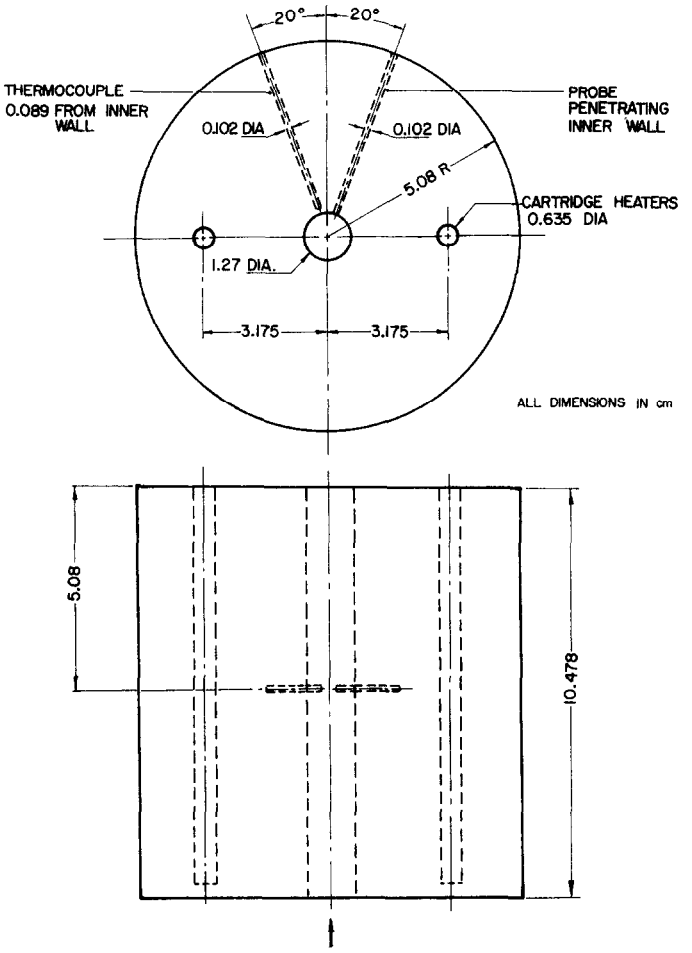

FIG. 3. Test section.

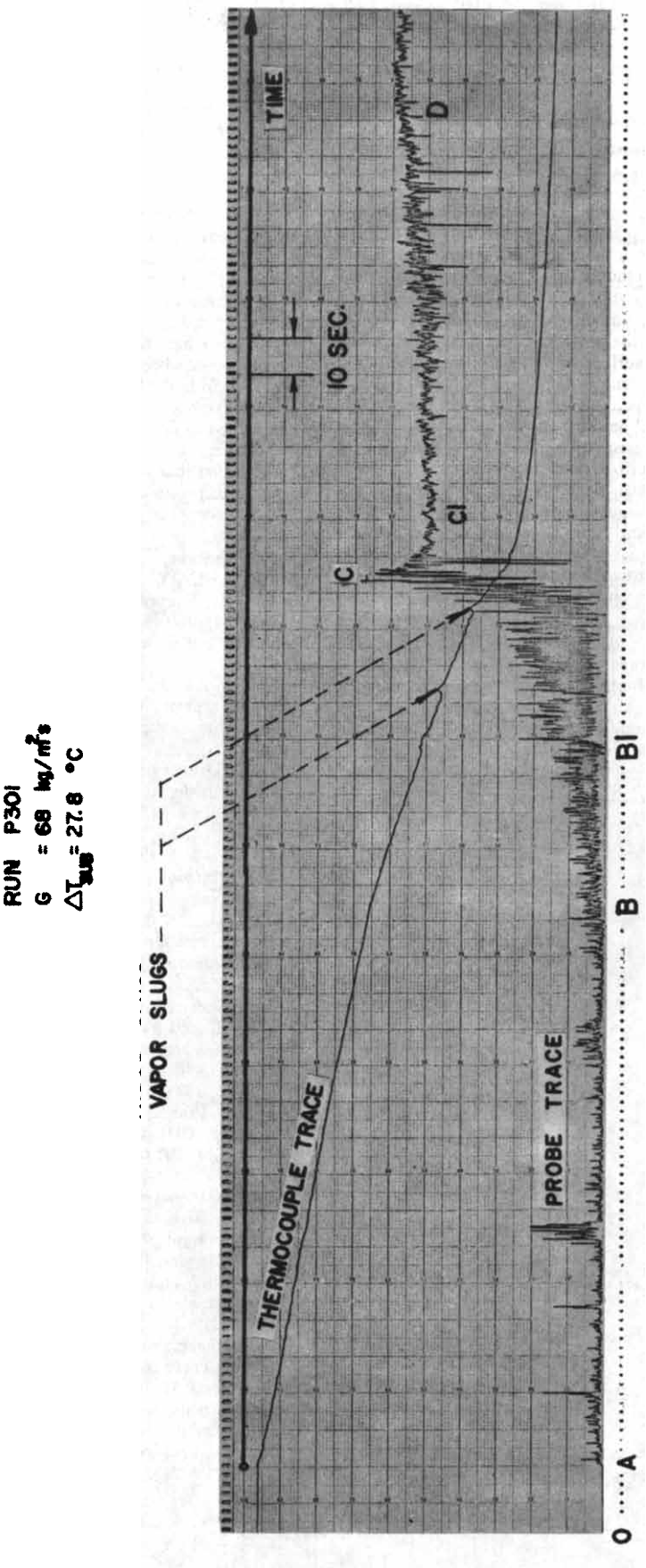

FIG. 4. Signals recorded from the probe and the thermocouple in flow boiling.

The test section is a part of a flow loop consisting of a hot water reservoir, flow meter pump and test section. Two glass tubes, installed at the inlet and exit of the test section, minimize test section heat losses and facilitate flow visualization. Further details of the experimental apparatus and procedures may be found in [3].

EXPERIMENTAL RESULTS

During each experiment the test section was initially heated to a temperature well in excess of the Leidenfrost temperature. The power was subsequently switched off and the coolant was introduced into the test section from the bottom.

Figure 4 shows an example of the probe signal and the adjacent thermocouple signal for a typical rewetting run. The probe signal was interpreted as follows:

(i) Momentary collisions of the liquid with the wall occur as evidenced from small fluctuations during the film boiling region AB. These are thought to be dry collisions where no wetting of the wall takes place [7]. The mean value of voltage fluctuations, as expected, is slightly higher than that of stagnant gas, as indicated in the region OA, before introducing the flow.

(ii) The region BC characterizes the transition boiling mode with momentary wetting being first detected at point B, followed by a more severe wetting after point B_1. Point B was selected because its mean value of voltage fluctuations started to deviate from that of film boiling region. During the period B_1C flow oscillations were observed at the glass test section due to the passage of vapor slugs which resulted in a sudden voltage drop and subsequent rise in wall temperatures as shown in Fig. 4. A slug flow was also observed by Bergles [8] at similar conditions.

(iii) Beyond point C, the voltage starts to stabilize signifying stable nucleate boiling where continuous liquid contact can take place.

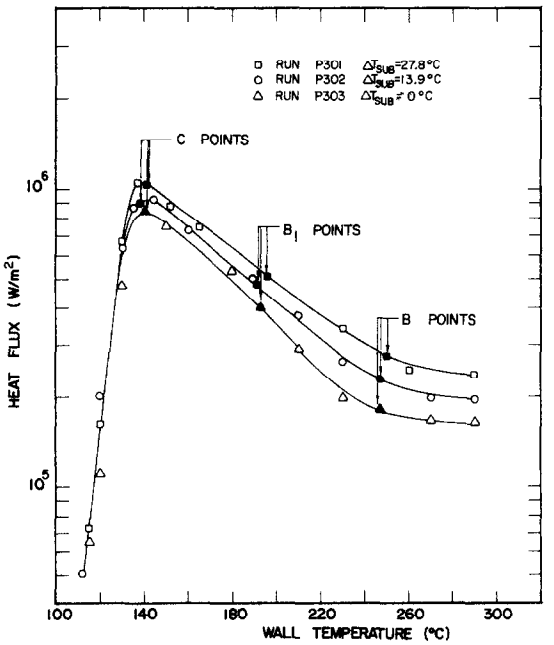

FIG. 5. Boiling curves of water for $G = 68\,kg/m^2\,s$.

Figure 5 presents some typical boiling curves of water for a mass flux of $68\,kg/m^2\,s$ with a subcooling varying from 0 to 28°C at atmospheric conditions. The experiments covered the mass flux range from 34 to $102\,kg/m^2\,s$. The boiling curves were derived from the temperature–time transients of the thermocouple adjacent to the probe using the technique developed in [9, 10]. The onset of intermittent wetting (point B) and the onset of continuous liquid contact (point C) as measured by the probe are also included for comparison.

CONCLUSIONS

The applicability of an electric resistance probe for detecting changes in boiling modes on a heated surface has been demonstrated under forced convective conditions. The probe made up from zirconium and platinum is suitable for continuous use even at high heated surface temperatures. The measured onset of intermittent wetting is very close to the minimum heat flux point from the boiling curve. The measured onset of continuous liquid contact coincides with CHF point from the boiling curve.

Although no obvious drift in probe voltage differential was noticed, such drift due to polarization has been observed in other studies using DC excitation. It is recommended that in future studies AC excitation be used to avoid this possible source of error.

Acknowledgements—The authors wish to express their gratitude to Dr. Y. Y. Hsu in suggesting the topic and to the Atomic Energy of Canada Limited and the U.S. Nuclear Regulatory Commission for providing financial support for this project.

REFERENCES

1. P. J. Berenson, Transition boiling heat transfer from a horizontal surface, MIT Technical Report No. 17 (1960).
2. D. C. Groeneveld and S. R. M. Gardiner, Post-CHF heat transfer under forced convective conditions, in *Proceedings, ASME Symposium on Nuclear Reactor Safety, Atlanta*, Vol. 1, pp. 43–74 (1977).
3. H. S. Ragheb, Development of electric probes to detect phase change at a heated surface, M.A.Sc. Thesis, University of Ottawa (1977).
4. Y. Iida and K. Kobayasi, An experimental investigation on the mechanism of pool boiling phenomena by a probe method, in *Proceedings of the 4th International Heat Transfer Conference*, Versailles, Vol. 5, Paper B1.3. Elsevier, Amsterdam (1970).
5. S. Wolf and D. H. Holmes, Critical heat flux in a sodium-heated steam generator tube, 17th National Heat Transfer Conference, Preprints A.I.Ch.E. Papers, pp. 275–282 (1977).
6. D. M. France, D. M. Carlson, T. Chiang and R. Priemer, CHF-induced thermal oscillations measured in an LMFBR steam generator tube wall, ANL-CT-78-1 (1977).
7. D. C. Groeneveld, The thermal behaviour of a heated surface at and beyond dryout, Atomic Energy of Canada Limited Report AECL-4309 (1972).
8. A. E. Bergles, R. F. Lopina and M. P. Fiori, Critical heat flux and flow pattern observations for low-pressure water flowing in tubes, *J. Heat Transfer* **89**, 69–74 (1967).
9. S. C. Cheng and K. T. Heng, A technique to construct a boiling curve from quenching data, *Letters Heat Mass Transfer* **3**, 413–420 (1976).
10. S. C. Cheng, K. T. Heng and W. Ng, A technique to construct a boiling curve from quenching data considering heat loss, *Int. J. Multiphase Flow* **3**, 495–499 (1977).